High-Pressure Chemistry

International Edition: DOI: 10.1002/anie.201504844
German Edition: DOI: 10.1002/ange.201504844

Rare-Earth-Metal Nitridophosphates through High-Pressure Metathesis

*Simon David Kloß and Wolfgang Schnick**

Abstract: *Developing a synthetic method to target an broad spectrum of unknown phases can lead to fascinating discoveries. The preparation of the first rare-earth-metal nitridophosphate $LiNdP_4N_8$ is reported. High-pressure solid-state metathesis between $LiPN_2$ and NdF_3 was employed to yield a highly crystalline product. The in situ formed LiF is believed to act both as the thermodynamic driving force and as a flux to aiding single-crystal formation in dimensions suitable for crystal structure analysis. Magnetic properties stemming from Nd^{3+} ions were measured by SQUID magnetometry. $LiNdP_4N_8$ serves as a model system for the exploration of rare-earth-metal nitridophosphates that may even be expanded to transition metals. High-pressure metathesis enables the systematic study of these uncharted regions of nitride-based materials with unprecedented properties.*

Nitridophosphates are believed to be one of the largest uncharted compound classes despite their proven structural versatility, which rivals even that of silicates, and their intriguing properties. Owing to their framework structure of PN_4 tetrahedra, nitridophosphates are closely related to silicates but they offer a broader structural diversity because of the possibility of triply bridging $N^{[3]}$ atoms.[1–4] To date, nitridophosphates of the first and second main groups have been thoroughly investigated. However, the number of hitherto discovered compounds (23 ternary ones, 15 structure types) is small when compared to the vast number of known silicate minerals,[5] but simultaneously highlights the potential for explorative chemistry. This general approach has been key to the discovery of high-performance materials, as demonstrated by the cuprate family of high T_c superconductors or the recent upsurge in perovskite-type solar cells.[6–8] Moreover, data-mining techniques have revealed that materials within the same structural family exhibit similar performances.[9] Hence the exploration of new materials families like nitridophosphates with transition or rare earth metals is anticipated to lead to the discovery of intriguing materials.

Nitridophosphate research has already produced functional materials like the clathrate $P_4N_4(NH)_4(NH_3)$, which is an open-framework structure hosting trapped ammonia molecules.[10] This clathrate has been discussed as a possible gas-storage material.[11] Furthermore, the zeolitic $Ba_3P_5N_{10}Br{:}Eu^{2+}$ is a promising luminescent material for solid-state lighting that emits natural white light.[12]

However, the accessibility of nitridophosphates through conventional solid-state synthesis is limited by the thermal stability of common starting materials like P_3N_5, which tend to decompose below the crystallization temperature of the targeted phases. High-pressure synthesis using the multianvil technique has promoted the exploration of alkaline earth nitridophosphates like MP_2N_4 (M = Be, Ca, Sr, Ba) and high-pressure polymorphs of the silica analogous PON.[13–17] However, the structural elucidation can be laborious owing to microcrystalline products that require elaborate powder diffraction and electron microscopy methods for structure determination.[14,16]

Synthetic success with alkali-metal and alkaline-earth-metal nitridophosphates could not yet be expanded to trivalent rare earth metals. In order to tackle the aforementioned problems, we tailored a new synthetic pathway by means of high-pressure metathesis and targeted rare-earth-metal nitridophosphates as a model system. Owing to their f electrons, such lanthanide materials offer more versatile properties, such as magnetism, than the already known nitridophosphates. We found that solid-state metathesis (SSM) is crucial for the preparation of rare-earth-metal nitridophosphates since it is imperative for phase formation and greatly aids crystal growth. SSM is an exchange reaction that capitalizes on the formation energy of a stable byproduct to generate the driving force for powering a less favored reaction. For example, rare-earth-metal nitridoborates, carbodiimides, and tetracyanoborates, as well as the functional materials GaN and Si_3N_4, are accessible by SSM.[18–20]

Herein, we report on the preparation of the first nitridophosphate with a trivalent cation, namely $LiNdP_4N_8$, by high-pressure metathesis. Stoichiometric amounts of NdF_3 and $LiPN_2$ were reacted at 5 GPa and approximately 1300 °C to yield $LiNdP_4N_8$ and LiF as described by the following equation [Eq. (1)].

$$NdF_3 + 4\,LiPN_2 \rightarrow LiNdP_4N_8 + 3\,LiF \qquad (1)$$

The reaction conditions were achieved through a 1000 t hydraulic press combined with a modified Walker-Type multianvil module.[21a–e] A colorless transparent product containing single crystals with a diameter of up to 100 μm was obtained after dissolving the byproduct LiF in H_2O (Figure S10 in the Supporting Information). The growth of such large crystals under high pressure can be attributed to in situ formed LiF, which is molten under these reaction conditions and can act as a flux.[22] The achievable crystal size easily exceeds the efficiency of the extrinsic mineralizer

---

[*] S. D. Kloß, Prof. Dr. W. Schnick
Department Chemie, Lehrstuhl für Anorganische Festkörperchemie
Ludwig-Maximilians-Universität München
Butenandtstrasse 5–13, 81377 München (Germany)
E-mail: wolfgang.schnick@uni-muenchen.de

Supporting information for this article is available on the WWW under http://dx.doi.org/10.1002/anie.201504844.

NH_4Cl, which was applied in the syntheses of β-HPN_2, β-$P_4N_6(NH)$, and γ-$P_4N_6(NH)$.[23–25]

The elemental composition, as determined by energy dispersive X-ray spectroscopy (EDX), is in good agreement with the theoretical atomic ratio of Nd/P/N = 1:4:8. Details of the EDX analysis can be found in Table S7 of the Supporting Information.

The crystal structure of $LiNdP_4N_8$ was solved in the orthorhombic space group *Pnma* (no. 62) from single-crystal X-ray diffraction data.[26] $LiNdP_4N_8$ crystallizes in a variant of the pseudo-orthorhombic structure of the mineral paracelsian ($BaAl_2Si_2O_8$, space group $P2_1/a$).[27] Additional information that rules out a monoclinic crustal system in $LiNdP_4N_8$ can be found in the Supporting Information. In order to quantify the similarity between paracelsian in an orthorhombic crystal system and $LiNdP_4N_8$, the two structures were compared by using the COMPSTRU tool of the Bilbao Crystallographic Server.[28] The mean shift of atomic positions is only 0.11 Å. The resulting measure of similarity Δ[29] of 0.073 emphasizes the close relation between the two structures.

The established structural model was confirmed by Rietveld refinement on X-ray powder diffraction data (Figure S2), which also indicates that $LiNdP_4N_8$ was prepared as a phase-pure compound. Further high-temperature powder diffraction experiments (Figure S5) reveal phase stability of at least 1000 °C in air, thus suggesting that $LiNdP_4N_8$ is not a high-pressure phase.

The structure of $LiNdP_4N_8$ consists of a network of all-side vertex-sharing PN_4 tetrahedra (Figure 1), which is best described as interconnected double crankshaft chains (Figure S4) running along [010]. These chains consist of stacked vierer rings (as defined by Liebau[5]) connected to adjacent layers by two up- and two down-pointing tetrahedra.[5] Li^+ and Nd^{3+} ions occupy the 4- and 8-ring channels running along *b* (Figure 1), with the 8-ring channels created by interconnection of the crankshaft chains. The framework topology is the same as in paracelsian and is characterized by the point symbol $\{4^2.6^3.8\}$, as calculated with TOPOS.[30,31] Because of the loop-branched double crankshaft chains, the paracelsian framework can be described by the Liebau classification $LiNd\{\boldsymbol{lb}1^3_\infty\}[P_4N_8]$.[5]

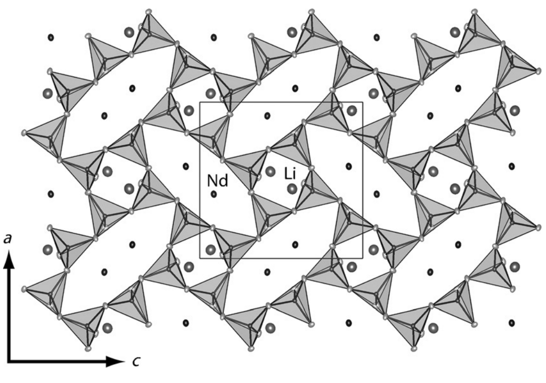

Figure 1. Projection of the $LiNdP_4N_8$ crystal structure along [010]. The unit cell is highlighted by black lines and the atoms are displayed with anisotropic displacement parameters set at 90% probability.

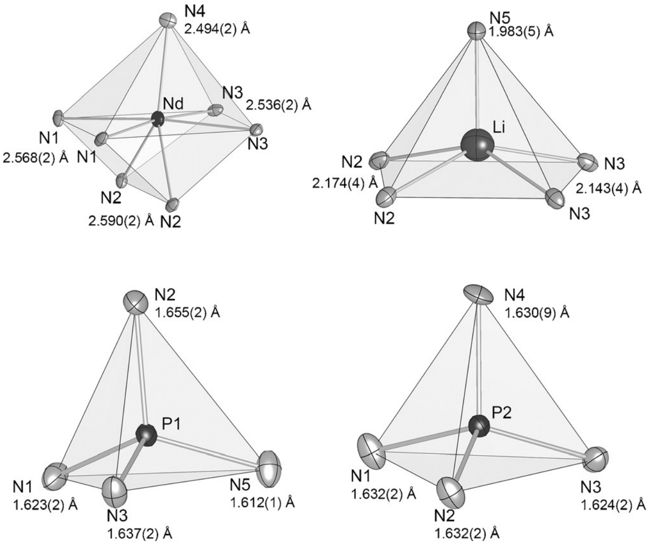

Figure 2. Coordination polyhedra around Nd, Li, P1, and P2. The thermal ellipsoids are set to 90% probability.

The 7-fold coordination sphere of Nd (Figure 2) is an augmented triangular prism with Nd–N distances of between 2.49 and 2.59 Å, which is in good agreement with the Nd–N distances in NdN (d(Nd–N) = 2.58 Å).[32] Li is coordinated in a slightly distorted square pyramid with Li–N distances ranging from 1.96 to 2.17 Å. This Li coordination polyhedron is unprecedented for nitrogen-containing framework structures and is only known within the complex structure of $Li_3Ni_4[NH_2]_{11}[NH_3]$.[33]

The FTIR spectrum of $LiNdP_4N_8$ (Figure S6) reveals characteristic P–N framework vibrations between 600–1500 cm^{-1}. The absence of N–H valence vibrations indicates that no N–H groups are contained in the sample.

Owing to the three unpaired electrons of Nd^{3+} (electron configuration $[Xe]4f^3$), SQUID magnetometry was employed to examine the magnetic properties of $LiNdP_4N_8$. The susceptibility data obtained at a constant magnetic field of 20 kOe follows the expected trend for paramagnetic substances in the range of 300 to 1.8 K (Figure 3). To calculate the

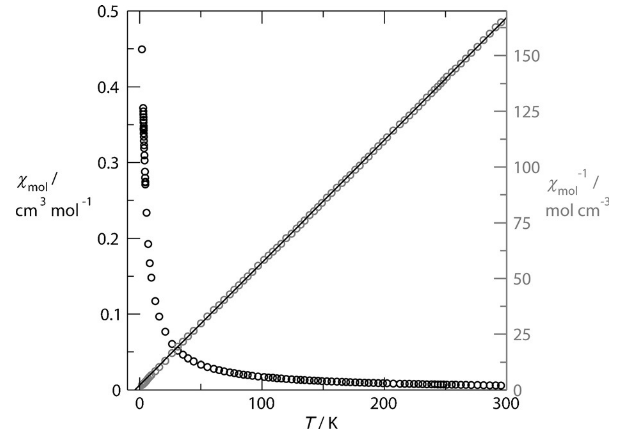

Figure 3. Susceptibility measurement carried out at 20 kOe. The data are displayed as χ_{mol} versus T (black circles) and χ_{mol}^{-1} versus T (gray circles). A linear regression (black line) was fit to the χ_{mol}^{-1} versus T data with the formula $y = 0.5494(4) + 2.20(8)$.

effective magnetic moment μ_{eff} with the Curie–Weiß law, a linear regression was fitted to the inverse molar susceptibility χ_{mol}^{-1} in the range of 300 to 50 K. The experimental μ_{eff} value of 3.815 μ_B is in good agreement with the theoretical value of 3.618 μ_B calculated from Hund's laws.[34] The Curie temperature Θ was determined to be −4 K, which is close to the theoretical value of 0 K. The deviations may stem from additional magnetic contributions caused by the amorphous phase visible in the powder pattern (Figure S2). Additionally, no magnetic ordering effects were observed in experiments with lower magnetic field strengths (Figure S7). $LiNdP_4N_8$ is thus the first confirmed paramagnetic nitridophosphate.

As mentioned above, we studied $LiNdP_4N_8$ as a model system to fathom the applicability of high-pressure metathesis in the development of new material families, in this case the rare-earth-metal nitridophosphates. We were able to demonstrate that this preparation method is capable of effortlessly producing a magnetic nitridophosphate with a trivalent cation. The synthetic complexity was deliberately kept minimalistic by the use of only two reactants, one of them commercially available, to emphasize the simplicity of this approach. However, the synthesis route can also be highly adaptive when the starting materials are carefully chosen. While the use of metal halides seems mandatory, the alkali-metal-containing compounds can be exchanged. For example, the degree of condensation of the PN_4 tetrahedral framework can be tuned by adding Li_3N as a reactant, which could result in compounds with the sum formula $LiLn_2PN_4$ that contain isolated PN_4 tetrahedra. Combined with the ability of high-pressure metathesis to grow single crystals, as demonstrated with $LiNdP_4N_8$, this flexibility enables rapid screening of a vast composition space. Fast structural elucidation is especially desired when searching for useful properties like body color, luminescence, or magnetism.

With the focus on exploring materials for general applications, it is advantageous to use compounds consisting of economical elements, such as transition metals.[9] Our high-pressure metathesis route is currently being expanded to metals such as iron, through which we hope to establish a gateway system to transition-metal nitridophosphates. Moreover, the idea of high-pressure metathesis can also be transferred to the structurally related family of nitridosilicates, since starting materials in the form of Li_2SiN_2 are readily available.[35] Transition-metal nitridosilicates are also a little explored substance class and may offer similar features to transition-metal nitridophosphates.

In conclusion, we prepared the first rare-earth-metal nitridophosphate $LiNdP_4N_8$ through high-pressure metathesis. The compound crystallizes in an undistorted orthorhombic variant of the paracelsian structure type, which is related to the feldspar type. By conducting a metathesis reaction, we were able to grow large single crystals at high pressure owing to the in situ formed mineralizer LiF. The growth of crystals suitable for X-ray crystallography greatly accelerates structure analysis. These results could form the basis for the discovery of a substantial number of interesting rare-earth- and transition-metal nitridophosphates, thereby stimulating progress in this exciting branch of chemistry.

Acknowledgements

We gratefully acknowledge financial support by the Fonds der Chemischen Industrie (FCI) and the Deutsche Forschungsgemeinschaft DFG. We gratefully acknowledge Roman Pobel for carrying out SQUID magnetometry.

Keywords: high-pressure chemistry · magnetic properties · metathesis · nitrides · rare earth metals

How to cite: *Angew. Chem. Int. Ed.* **2015**, *54*, 11250–11253
Angew. Chem. **2015**, *127*, 11402–11405

---

[1] A. Stock, H. Grüneberg, *Ber. Dtsch. Chem. Ges.* **1907**, *40*, 2573–2578.
[2] S. Horstmann, E. Irran, W. Schnick, *Angew. Chem. Int. Ed. Engl.* **1997**, *36*, 1873–1875; *Angew. Chem.* **1997**, *109*, 1938–1940.
[3] S. Horstmann, E. Irran, W. Schnick, *Z. Anorg. Allg. Chem.* **1998**, *624*, 620–628.
[4] S. Horstmann, E. Irran, W. Schnick, *Angew. Chem. Int. Ed. Engl.* **1997**, *36*, 1992–1994; *Angew. Chem.* **1997**, *109*, 2085–2087.
[5] F. Liebau, *Structural Chemistry of Silicates: Structure, Bonding, and Classification*, Springer, Berlin, **1985**.
[6] J. G. Bednorz, K. A. Müller, *Z. Phys. B* **1986**, *64*, 189–193.
[7] M. K. Wu, J. R. Ashburn, C. J. Torng, P. H. Hor, R. L. Meng, L. Gao, Z. J. Huang, Y. Q. Wang, C. W. Chu, *Phys. Rev. Lett.* **1987**, *58*, 908–910.
[8] H. J. Snaith, *J. Phys. Chem. Lett.* **2013**, *4*, 3623–3630.
[9] M. W. Gaultois, T. D. Sparks, C. K. H. Borg, R. Seshadri, W. D. Bonificio, D. R. Clarke, *Chem. Mater.* **2013**, *25*, 2911–2920.
[10] F. Karau, W. Schnick, *Angew. Chem. Int. Ed.* **2006**, *45*, 4505–4508; *Angew. Chem.* **2006**, *118*, 4617–4620.
[11] M. Pouchard, *Nature* **2006**, *442*, 878–879.
[12] A. Marchuk, W. Schnick, *Angew. Chem. Int. Ed.* **2015**, *54*, 2383–2387; *Angew. Chem.* **2015**, *127*, 2413–2417.
[13] F. W. Karau, W. Schnick, *J. Solid State Chem.* **2005**, *178*, 135–141.
[14] D. Baumann, S. J. Sedlmaier, W. Schnick, *Angew. Chem. Int. Ed.* **2012**, *51*, 4707–4709; *Angew. Chem.* **2012**, *124*, 4785–4787.
[15] F. J. Pucher, S. R. Römer, F. W. Karau, W. Schnick, *Chem. Eur. J.* **2010**, *16*, 7208–7214.
[16] F. W. Karau, L. Seyfarth, O. Oeckler, J. Senker, K. Landskron, W. Schnick, *Chem. Eur. J.* **2007**, *13*, 6841–6852.
[17] F. J. Pucher, A. Marchuk, P. J. Schmidt, D. Wiechert, W. Schnick, *Chem. Eur. J.* **2015**, *21*, 6443–6448.
[18] H. J. Meyer, *Dalton Trans.* **2010**, *39*, 5973–5982.
[19] C. H. Wallace, S. H. Kim, G. Rose, L. Rao, J. R. Heath, M. Nicol, R. B. Kaner, *Appl. Phys. Lett.* **1998**, *72*, 596–598.
[20] M. P. Shemkunas, G. H. Wolf, K. Leinenweber, W. T. Petuskey, *J. Am. Ceram. Soc.* **2004**, *85*, 101–104.
[21] a) N. Kawai, S. Endo, *Rev. Sci. Instrum.* **1970**, *41*, 1178–1181; b) D. Walker, M. A. Carpenter, C. M. Hitch, *Am. Mineral.* **1990**, *75*, 1020–1028; c) D. Walker, *Am. Mineral.* **1991**, *76*, 1092–1100; d) D. C. Rubie, *Phase Transitions* **1999**, *68*, 431–451; e) H. Huppertz, *Z. Kristallogr.* **2004**, *219*, 330–338.
[22] I. Jackson, *Phys. Earth Planet. Inter.* **1977**, *14*, 86–94.
[23] D. Baumann, W. Schnick, *Inorg. Chem.* **2014**, *53*, 7977–7982.
[24] D. Baumann, W. Schnick, *Angew. Chem. Int. Ed.* **2014**, *53*, 14490–14493; *Angew. Chem.* **2014**, *126*, 14718–14721.
[25] A. Marchuk, F. J. Pucher, F. W. Karau, W. Schnick, *Angew. Chem. Int. Ed.* **2014**, *53*, 2469–2472; *Angew. Chem.* **2014**, *126*, 2501–2504.
[26] Crystal data for $LiNdP_4N_8$: crystal size $0.020\times0.030\times0.030$ mm^3, space group *Pnma* (no. 62), $a=8.7305(17)$, $b=7.8783(16)$, $c=9.0881(18)$ Å, $V=625.1(2)$ Å^3, $Z=4$, $\rho_{diffm}=4.114$ g cm^{-3}, Bruker D8 Venture, Mo-K$_\alpha$-radiation (71.073 pm), multiscan

absorption correction, 12131 reflections, 1262 independent reflections, least squares refinement on F^2, R-values (all data/ $F_0^2 \geq 2\sigma(F_0^2)$): $R_1 = 0.0135/0.0128$, $wR_2 = 0.0343/0.0341$, GooF = 1.159 for 1224 observed reflections ($F_0^2 \geq 2\sigma(F_0^2)$) and 70 parameters. Further details on the crystal structure investigations may be obtained from the Fachinformationszentrum Karlsruhe, 76344 Eggenstein-Leopoldshafen, Germany (fax: (+49)7247-808-666; e-mail: crysdata@fiz-karlsruhe.de), on quoting the depository number CSD-429542.

[27] J. V. Smith, *Acta Crystallogr.* **1953**, *6*, 613–620.

[28] E. S. Tasci, G. de La Flor, D. Orobengoa, C. Capillas, M. Perez-Mato, M. I. Aroyo, *EPJ Web Conf.* **2012**, *22*, 00009.

[29] G. Bergerhoff, M. Berndt, K. Brandenburg, T. Degen, *Acta Crystallogr. Sect. B* **1999**, *55*, 147–156.

[30] V. A. Blatov, *IUCr CompComm Newsl.* **2006**, *7*, 4–38.

[31] V. A. Blatov, M. O'Keeffe, D. M. Proserpio, *CrystEngComm* **2010**, *12*, 44–48.

[32] W. Klemm, G. Winkelmann, *Z. Anorg. Allg. Chem.* **1956**, *288*, 87–90.

[33] A. Tenten, H. Jacobs, *J. Alloys Compd.* **1991**, *177*, 193–217.

[34] F. Hund, *Z. Phys.* **1925**, *33*, 855–859.

[35] S. Pagano, M. Zeuner, S. Hug, W. Schnick, *Eur. J. Inorg. Chem.* **2009**, 1579–1584.

Received: May 28, 2015